UNCERTAINTY QUANTIFICATION FOR JOINT INPUT-STATE ESTIMATION IN STRUCTURAL DYNAMICS

K. Maes[1], A.W. Smyth[2], G. De Roeck[1], and G. Lombaert[1]

[1]KU Leuven, Department of Civil Engineering
Kasteelpark Arenberg 40, B-3001 Leuven, Belgium
e-mail: {kristof.maes,guido.deroeck,geert.lombaert}@bwk.kuleuven.be

[2]Columbia University, Deptartment of Civil Engineering and Engineering Mechanics
610 S.W. Mudd Building, NY 10027, New York, USA
e-mail: smyth@civil.columbia.edu

Keywords: Uncertainty Quantification, Joint Input-State Estimation, Force Identification, Response Estimation, Stochastic Excitation.

Abstract. *This paper presents a novel approach for quantification of the estimation uncertainty on the results obtained from joint input-state estimation in structural dynamics. The uncertainty accounted for originates from measurement errors and unknown stochastic excitation, that is acting on the structure besides the forces that are to be identified. The uncertainty quantification approach is applied for a joint input-state estimation algorithm that is used for force identification and response estimation in structural dynamics. The approach can, however, be extended to other force and state estimation algorithms. The uncertainty on the estimated quantities can be used to design a sensor network and to determine the optimal noise statistics that are applied for joint input-state estimation. The uncertainty quantification approach is verified using numerical simulations.*

1 Introduction

Accurate online reconstruction of the dynamic forces acting on a structure and its corresponding response behavior, referred to as the system state, are of great importance to many engineering applications. Very often the input, i.e. the dynamic forces, cannot be measured directly, e.g. for wind loads, whereas the response of the structure cannot be measured at all physical locations, due to practical and economical considerations. In these cases, the forces and system states have to be determined indirectly from dynamic measurements of the response using system inversion techniques, and can be used to extrapolate the response to unmeasured locations.

The paper presents a novel approach for quantification of the estimation uncertainty on the results obtained from joint input-state estimation in structural dynamics. The uncertainty originates from measurement errors and unknown stochastic excitation, that is acting on the structure besides the forces that are to be identified. The uncertainty quantification approach is applied for a Kalman filter based joint input-state estimation algorithm. The algorithm was originally proposed by Gillijns and De Moor in [2], was then introduced in structural dynamics by Lourens et al. in [4], and was further extended by Maes et al. in [6]. The uncertainty quantification approach can be easily extended to other force and state estimation algorithms presented in the literature, e.g. [3, 8, 9]. The uncertainty quantification approach is verified using numerical simulations.

The outline of the paper is as follows. Section 2 presents the mathematical formulation, which includes the joint input-state estimation algorithm and the approach to calculate the uncertainty introduced by unknown stochastic excitation and measurement errors. Section 3 shows a verification of the proposed methodology, using numerical simulations. Finally, in Section 4, the work is concluded.

2 MATHEMATICAL FORMULATION

2.1 System model

In structural dynamics, first principles models, e.g. finite element (FE) models, are widely used. In many cases, modally reduced order models are applied, constructed from a limited number of structural modes. When proportional damping is assumed, the continuous-time decoupled equations of motion for modally reduced order models are given by:

$$\ddot{\mathbf{z}}(t) + \mathbf{\Gamma}\dot{\mathbf{z}}(t) + \mathbf{\Omega}^2\mathbf{z}(t) = \mathbf{\Phi}^{\mathrm{T}}\mathbf{S}_{\mathrm{p}}(t)\mathbf{p}(t) \tag{1}$$

where $\mathbf{z}(t) \in \mathbb{R}^{n_{\mathrm{m}}}$ is the vector of modal coordinates, with n_{m} the number of modes taken into account in the model. The excitation force is written as the product of a matrix $\mathbf{S}_{\mathrm{p}}(t) \in \mathbb{R}^{n_{\mathrm{dof}} \times n_{\mathrm{p}}}$, specifying the force locations, and a time history vector $\mathbf{p}(t) \in \mathbb{R}^{n_{\mathrm{p}}}$, with n_{p} the number of forces. For the remainder of this paper, the matrix $\mathbf{S}_{\mathrm{p}}(t)$ is assumed to be time-invariant. The results, however, can be readily extended to the case where $\mathbf{S}_{\mathrm{p}}(t)$ is varying with time. The number of degrees of freedom is denoted by n_{dof}. $\mathbf{\Gamma} \in \mathbb{R}^{n_{\mathrm{m}} \times n_{\mathrm{m}}}$ is a diagonal matrix containing the terms $2\xi_j\omega_j$ on its diagonal, where ω_j and ξ_j are the natural frequency and modal damping ratio corresponding to mode j, respectively. $\mathbf{\Omega} \in \mathbb{R}^{n_{\mathrm{m}} \times n_{\mathrm{m}}}$ is a diagonal matrix as well, containing the natural frequencies ω_j on its diagonal, and $\mathbf{\Phi} \in \mathbb{R}^{n_{\mathrm{dof}} \times n_{\mathrm{m}}}$ is a matrix containing the mass normalized mode shapes ϕ_j as columns.

The decoupled governing equations can be written in state-space form, which after time discretization reads:

$$\mathbf{x}_{[k+1]} = \mathbf{A}\mathbf{x}_{[k]} + \mathbf{B}\mathbf{p}_{[k]} \tag{2}$$

where $\mathbf{x}_{[k]} = \mathbf{x}(k\Delta t)$ and $\mathbf{p}_{[k]} = \mathbf{p}(k\Delta t)$, $k = 1, \ldots, N$, Δt is the sampling time step, and N is the total number of samples. The state vector $\mathbf{x}_{[k]}$ consists of the modal displacements and velocities:

$$\mathbf{x}_{[k]} = \begin{bmatrix} \mathbf{z}_{[k]} \\ \dot{\mathbf{z}}_{[k]} \end{bmatrix} \tag{3}$$

When applying a zero order hold assumption on the input vector $\mathbf{p}_{[k]}$, the expressions for the state-feedback matrix $\mathbf{A}$ and the state-input matrix $\mathbf{B}$ in Eq. (2) are given by:

$$\mathbf{A} = \exp\left(\begin{bmatrix} \mathbf{0} & \mathbf{I}_{n_{\mathrm{m}}} \\ -\mathbf{\Omega}^2 & -\mathbf{\Gamma} \end{bmatrix} \Delta t \right) \tag{4}$$

$$\mathbf{B} = \left(\mathbf{A} - \mathbf{I}_{n_{\mathrm{s}}} \right) \begin{bmatrix} \mathbf{0} & \mathbf{I}_{n_{\mathrm{m}}} \\ -\mathbf{\Omega}^2 & -\mathbf{\Gamma} \end{bmatrix}^{-1} \begin{bmatrix} \mathbf{0} \\ \mathbf{\Phi}^{\mathrm{T}}\mathbf{S}_{\mathrm{p}} \end{bmatrix} \tag{5}$$

where $\mathbf{I}_{n_{\mathrm{m}}} \in \mathbb{R}^{n_{\mathrm{m}} \times n_{\mathrm{m}}}$ and $\mathbf{I}_{n_{\mathrm{s}}} \in \mathbb{R}^{n_{\mathrm{s}} \times n_{\mathrm{s}}}$ are identity matrices. The reader is referred to [1] for a detailed overview of common time discretization schemes. As an alternative to models based on first principles, models can be directly identified from experimental vibration data using system identification techniques, see e.g. [10, 11, 13].

The output vector $\mathbf{d}(t) \in \mathbb{R}^{n_{\mathrm{d}}}$ is generally written as:

$$\mathbf{d}(t) = \mathbf{S}_{\mathrm{d,a}}\mathbf{\Phi}\ddot{\mathbf{z}}(t) + \mathbf{S}_{\mathrm{d,v}}\mathbf{\Phi}\dot{\mathbf{z}}(t) + \mathbf{S}_{\mathrm{d,d}}\mathbf{\Phi}\mathbf{z}(t) \tag{6}$$

where $\mathbf{S}_{\mathrm{d,a}}$, $\mathbf{S}_{\mathrm{d,v}}$, and $\mathbf{S}_{\mathrm{d,d}} \in \mathbb{R}^{n_{\mathrm{d}} \times n_{\mathrm{dof}}}$ are matrices relating the measured accelerations, velocities and displacements or strains, respectively, to the degrees of freedom in the model. The output vector is composed of $n_{\mathrm{d,d}}$ displacement or strain measurements, $n_{\mathrm{d,v}}$ velocity measurements and $n_{\mathrm{d,a}}$ acceleration measurements, where n_{d} is the sum of $n_{\mathrm{d,d}}$, $n_{\mathrm{d,v}}$, and $n_{\mathrm{d,a}}$.

Eq. (6) is transformed into its state-space form, using Eq. (1):

$$\mathbf{d}_{[k]} = \mathbf{G}\mathbf{x}_{[k]} + \mathbf{J}\mathbf{p}_{[k]} \tag{7}$$

where $\mathbf{d}_{[k]} = \mathbf{d}(k\Delta t)$. The expressions for the state-output matrix $\mathbf{G}$ and the direct transmission matrix $\mathbf{J}$ do in general not depend on the time discretization scheme, because Eqs. (6) and (7) do not involve a time lag. The expressions for $\mathbf{G}$ and $\mathbf{J}$ are given by:

$$\mathbf{G} = \begin{bmatrix} \mathbf{S}_{\mathrm{d,d}}\mathbf{\Phi} - \mathbf{S}_{\mathrm{d,a}}\mathbf{\Phi}\mathbf{\Omega}^2 & \mathbf{S}_{\mathrm{d,v}}\mathbf{\Phi} - \mathbf{S}_{\mathrm{d,a}}\mathbf{\Phi}\mathbf{\Gamma} \end{bmatrix} \tag{8}$$

$$\mathbf{J} = \begin{bmatrix} \mathbf{S}_{\mathrm{d,a}}\mathbf{\Phi}\mathbf{\Phi}^{\mathrm{T}}\mathbf{S}_{\mathrm{p}} \end{bmatrix} \tag{9}$$

The force vector $\mathbf{p}_{[k]}$ in Eqs. (2) and (7) corresponds to the forces acting on the structure that are to be estimated. In addition, unknown additional forces are acting on the structure, assumed to be stochastic. This additional stochastic excitation, as well as measurement errors and modeling errors, are accounted for in the system model by stochastic noise processes, i.e. process noise $\mathbf{w}_{[k]}$ and measurement noise $\mathbf{v}_{[k]}$. When

the noise processes are added to Eqs. (2) and (7), the following discrete-time combined deterministic-stochastic state-space description of the system is obtained:

$$\mathbf{x}_{[k+1]} = \mathbf{A}\mathbf{x}_{[k]} + \mathbf{B}\mathbf{p}_{[k]} + \mathbf{w}_{[k]} \tag{10}$$

$$\mathbf{d}_{[k]} = \mathbf{G}\mathbf{x}_{[k]} + \mathbf{J}\mathbf{p}_{[k]} + \mathbf{v}_{[k]} \tag{11}$$

where $\mathbf{x}_{[k]} \in \mathbb{R}^{n_s}$ is the state vector, $\mathbf{d}_{[k]} \in \mathbb{R}^{n_d}$ is the measured output vector, and $\mathbf{p}_{[k]} \in \mathbb{R}^{n_p}$ is the input vector, to be estimated, with n_s the number of system states, n_d the number of outputs, and n_p the number of inputs. The process noise vector $\mathbf{w}_{[k]} \in \mathbb{R}^{n_s}$ and measurement noise vector $\mathbf{v}_{[k]} \in \mathbb{R}^{n_d}$ generally account for unknown stochastic excitation and modeling errors. In addition, the measurement noise vector $\mathbf{v}_{[k]}$ accounts for measurement errors. The process noise vectors due to stochastic excitation and modeling errors are denoted by $\mathbf{w}_{S[k]}$ and $\mathbf{w}_{E[k]}$, respectively. The measurement noise vectors due to stochastic excitation, measurement errors, and modeling errors, are denoted by $\mathbf{v}_{S[k]}$, $\mathbf{v}_{M[k]}$, and $\mathbf{v}_{E[k]}$, respectively. The following expressions are obtained:

$$\mathbf{w}_{[k]} = \mathbf{w}_{S[k]} + \mathbf{w}_{E[k]} \tag{12}$$

$$\mathbf{v}_{[k]} = \mathbf{v}_{S[k]} + \mathbf{v}_{M[k]} + \mathbf{v}_{E[k]} \tag{13}$$

The vectors $\mathbf{w}_{S[k]}$ and $\mathbf{v}_{S[k]}$ corresponding to the stochastic excitation are given by:

$$\mathbf{w}_{S[k]} = \mathbf{B}'\mathbf{p}_{S[k]} \tag{14}$$

$$\mathbf{v}_{S[k]} = \mathbf{J}'\mathbf{p}_{S[k]} \tag{15}$$

where $\mathbf{p}_{S[k]} \in \mathbb{R}^{n_{PS}}$ is the vector of stochastic forces acting on the structure, and the matrices $\mathbf{B}' \in \mathbb{R}^{n_s \times n_{PS}}$ and $\mathbf{J}' \in \mathbb{R}^{n_d \times n_{PS}}$ relate the state vector $\mathbf{x}_{[k+1]}$ and the output vector $\mathbf{d}_{[k]}$ to the vector of stochastic forces $\mathbf{p}_{S[k]}$, respectively.

Consider in addition a vector $\mathbf{d}_e(t) \in \mathbb{R}^{n_{d_e}}$ of output quantities that are to be identified from the measured data and the system model, hereafter referred to as the vector of extrapolated output quantities:

$$\mathbf{d}_e(t) = \mathbf{S}_{d_e,a}\boldsymbol{\Phi}\ddot{\mathbf{z}}(t) + \mathbf{S}_{d_e,v}\boldsymbol{\Phi}\dot{\mathbf{z}}(t) + \mathbf{S}_{d_e,d}\boldsymbol{\Phi}\mathbf{z}(t) \tag{16}$$

where the matrices $\mathbf{S}_{d_e,a}$, $\mathbf{S}_{d_e,v}$, and $\mathbf{S}_{d_e,d} \in \mathbb{R}^{n_{d_e} \times n_{dof}}$ relate the identified accelerations, velocities and displacements or strains, respectively, to the degrees of freedom in the model (see also Eq. (6)). After transformation of Eq. (16) into its state-space form, using Eq. (1), and adding measurement noise, the following (discrete-time) output equation corresponding to the extrapolated output quantities is obtained:

$$\mathbf{d}_{e[k]} = \mathbf{G}_e\mathbf{x}_{[k]} + \mathbf{J}_e\mathbf{p}_{[k]} + \mathbf{v}_{e[k]} \tag{17}$$

The matrices $\mathbf{G}_e \in \mathbb{R}^{n_{d_e} \times n_s}$ and $\mathbf{J}_e \in \mathbb{R}^{n_{d_e} \times n_p}$ are obtained from Eqs. (8) and (9), respectively, by replacing the selection matrices $\mathbf{S}_{d,a}$, $\mathbf{S}_{d,v}$, and $\mathbf{S}_{d,d}$ with the matrices $\mathbf{S}_{d_e,a}$, $\mathbf{S}_{d_e,v}$, and $\mathbf{S}_{d_e,d}$, respectively. The measurement noise vector $\mathbf{v}_{e[k]}$ in Eq. (17) accounts for stochastic excitation and modeling errors and is therefore generally written as:

$$\mathbf{v}_{e[k]} = \mathbf{J}'_e\mathbf{p}_{S[k]} + \mathbf{v}_{eE[k]} \tag{18}$$

where the matrix $\mathbf{J}'_e \in \mathbb{R}^{n_{d_e} \times n_{PS}}$ relates the extrapolated output vector $\mathbf{d}_{e[k]}$ to the vector of stochastic forces $\mathbf{p}_{S[k]}$, and $\mathbf{v}_{eE[k]}$ is the component of $\mathbf{v}_{e[k]}$ due to modeling errors.

Under the assumption of stationary noise processes, the stochastic forces $\mathbf{p}_{S[k]}$ are characterized by the autocorrelation (AC) function $\mathbf{R}_{p_S p_S}(\tau)$ and corresponding Power Spectral Density (PSD) function $\mathbf{S}_{p_S p_S}(\omega)$, that form the Wiener-Khinchin transformation pair:

$$\mathbf{R}_{p_S p_S}(\tau) \equiv \mathbb{E}\{\mathbf{p}_S(t+\tau)\mathbf{p}_S^T(t)\} = \frac{1}{2\pi} \int_{-\infty}^{+\infty} \mathbf{S}_{p_S p_S}(\omega)\exp(i\omega\tau)d\omega \qquad (19)$$

$$\mathbf{S}_{p_S p_S}(\omega) = \int_{-\infty}^{+\infty} \mathbf{R}_{p_S p_S}(\tau)\exp(-i\omega\tau)d\tau \qquad (20)$$

where $i = \sqrt{-1}$. The discrete AC $\mathbf{R}_{p_S p_S[l]}$ is obtained as $\mathbf{R}_{p_S p_S}(l\Delta t)$, with l the time lag and Δt the sampling time step. In case the stochastic forces correspond to finite bandwidth white noise, the AC $\mathbf{R}_{p_S p_S[l]}$ and PSD $\mathbf{S}_{p_S p_S}(\omega_n)$ are given by:

$$\mathbf{R}_{p_S p_S[l]} = \mathbf{C}_p \delta_{[l]} \qquad (21)$$

$$\mathbf{S}_{p_S p_S}(\omega_n) = \mathbf{C}_p/F \qquad (22)$$

where $\mathbf{C}_p \in \mathbb{R}^{n_{ps} \times n_{ps}}$ is the covariance matrix of the stochastic forces, e.g. $\sigma_{p_S}^2 \mathbf{I}_{n_{ps}}$ for n_{ps} independent stochastic forces with equal standard deviation σ_{p_S}. F is the sampling frequency (in Hz) used in the discretization process, $\omega_n = 2\pi(n-1)/(N\Delta t)$, and $\delta_{[l]} = 1$ for $l = 0$ and 0 otherwise.

The measurement errors $\mathbf{v}_{M[k]}$ are defined similarly by the AC $\mathbf{R}_{v_M v_M[l]}$ and corresponding PSD $\mathbf{S}_{v_M v_M}(\omega_n)$, which, in case the measurement errors for all output signals correspond to finite bandwidth white noise, are given by:

$$\mathbf{R}_{v_M v_M[l]} = \mathbf{R}_M \delta_{[l]} \qquad (23)$$

$$\mathbf{S}_{v_M v_M}(\omega_n) = \mathbf{R}_M/F \qquad (24)$$

where $\mathbf{R}_M \in \mathbb{R}^{n_d \times n_d}$ is the measurement error covariance matrix.

2.2 Joint input-state estimation algorithm

Throughout the derivation of the joint input-state estimation algorithm in [6], the system matrices $\mathbf{A}$, $\mathbf{B}$, $\mathbf{G}$, $\mathbf{J}$, $\mathbf{G}_e$, and $\mathbf{J}_e$ are assumed known. In addition, it is assumed that the sensor network meets the conditions for instantaneous system inversion derived in [5]. The noise processes $\mathbf{w}_{[k]}$ and $\mathbf{v}_{[k]}$ are assumed to be zero mean and white, with known covariance matrices $\mathbf{Q}$, $\mathbf{R}$, and $\mathbf{S}$, defined by:

$$\mathbb{E}\left[\begin{pmatrix}\mathbf{w}_{[k]} \\ \mathbf{v}_{[k]}\end{pmatrix}\begin{pmatrix}\mathbf{w}_{[l]}^T & \mathbf{v}_{[l]}^T\end{pmatrix}\right] = \begin{bmatrix}\mathbf{Q} & \mathbf{S} \\ \mathbf{S}^T & \mathbf{R}\end{bmatrix}\delta_{[k-l]} \qquad (25)$$

with $\mathbf{R} > 0$, $\begin{bmatrix}\mathbf{Q} & \mathbf{S} \\ \mathbf{S}^T & \mathbf{R}\end{bmatrix} \geq 0$.

The noise process $\mathbf{v}_{e[k]}$ is assumed to be zero mean and white, with known covariance matrices $\mathbf{R}_e$ and $\mathbf{R}_c$, defined by:

$$\mathbb{E}\left[\mathbf{v}_{e[k]}\mathbf{v}_{e[l]}^T\right] = \mathbf{R}_e \delta_{[k-l]}, \text{ and } \mathbb{E}\left[\mathbf{v}_{e[k]}\mathbf{v}_{[l]}^T\right] = \mathbf{R}_c \delta_{[k-l]} \qquad (26)$$

When the data vector includes accelerations and the noise processes $\mathbf{w}_{[k]}$ and $\mathbf{v}_{[k]}$ account for additional stochastic forces, other than the ones included in the input vector $\mathbf{p}_{[k]}$, the process noise and measurement noise are inherently correlated [7] (i.e. $\mathbf{S} \neq \mathbf{0}$). This correlation is not accounted for in the original joint input-state estimation algorithm proposed in [2], but is accounted for in the algorithm proposed in [6]. The joint input-state estimation algorithm proposed in [6] is outlined next.

Joint input-state estimation consists of estimating the forces $\mathbf{p}_{[k]}$ and states $\mathbf{x}_{[k]}$, from a set of response measurements $\mathbf{d}_{[k]}$. A state estimate $\hat{\mathbf{x}}_{[k|l]}$ is defined as an estimate of $\mathbf{x}_{[k]}$, given the output sequence $\mathbf{d}_{[n]}$, with $n = 0, 1, \ldots, l$. The corresponding error covariance matrix, denoted by $\mathbf{P}_{\mathrm{x}[k|l]}$, is defined as:

$$\mathbf{P}_{\mathrm{x}[k|l]} \equiv \mathbb{E}\left\{(\mathbf{x}_{[k]} - \hat{\mathbf{x}}_{[k|l]})(\mathbf{x}_{[k]}^{\mathrm{T}} - \hat{\mathbf{x}}_{[k|l]}^{\mathrm{T}})\right\} \tag{27}$$

where $\mathbb{E}\{\cdot\}$ indicates the expectation operator. An input estimate $\hat{\mathbf{p}}_{[k|l]}$ and its error covariance matrix $\mathbf{P}_{\mathrm{p}[k|l]}$ are defined similarly. The cross covariance matrices $\mathbf{P}_{\mathrm{xp}[k|l]}$ and $\mathbf{P}_{\mathrm{px}[k|l]}$ are defined as:

$$\mathbf{P}_{\mathrm{xp}[k|l]} = \mathbf{P}_{\mathrm{px}[k|l]}^{\mathrm{T}} \equiv \mathbb{E}\left\{(\mathbf{x}_{[k]} - \hat{\mathbf{x}}_{[k|l]})(\mathbf{p}_{[k]}^{\mathrm{T}} - \hat{\mathbf{p}}_{[k|l]}^{\mathrm{T}})\right\} \tag{28}$$

The filtering algorithm is initialized using an initial state estimate vector $\hat{\mathbf{x}}_{[0|-1]}$ and its error covariance matrix $\mathbf{P}_{\mathrm{x}[0|-1]}$. The estimate $\hat{\mathbf{x}}_{[0|-1]}$ is assumed unbiased and independent of the noise processes $\mathbf{w}_{[k]}$ and $\mathbf{v}_{[k]}$ for all k. The algorithm proceeds by computing the force and state estimates recursively in three steps, i.e. the input estimation step, the measurement update and the time update:

Input estimation

$$\tilde{\mathbf{R}}_{[k]} = \mathbf{G}\mathbf{P}_{\mathrm{x}[k|k-1]}\mathbf{G}^{\mathrm{T}} + \mathbf{R} \tag{29}$$

$$\mathbf{M}_{[k]} = \left(\mathbf{J}^{\mathrm{T}}\tilde{\mathbf{R}}_{[k]}^{-1}\mathbf{J}\right)^{-1}\mathbf{J}^{\mathrm{T}}\tilde{\mathbf{R}}_{[k]}^{-1} \tag{30}$$

$$\hat{\mathbf{p}}_{[k|k]} = \mathbf{M}_{[k]}\left(\mathbf{d}_{[k]} - \mathbf{G}\hat{\mathbf{x}}_{[k|k-1]}\right) \tag{31}$$

$$\mathbf{P}_{\mathrm{p}[k|k]} = \left(\mathbf{J}^{\mathrm{T}}\tilde{\mathbf{R}}_{[k]}^{-1}\mathbf{J}\right)^{-1} \tag{32}$$

Measurement update

$$\mathbf{K}_{[k]} = \mathbf{P}_{\mathrm{x}[k|k-1]}\mathbf{G}^{\mathrm{T}}\tilde{\mathbf{R}}_{[k]}^{-1} \tag{33}$$

$$\hat{\mathbf{x}}_{[k|k]} = \hat{\mathbf{x}}_{[k|k-1]} + \mathbf{K}_{[k]}\left(\mathbf{d}_{[k]} - \mathbf{G}\hat{\mathbf{x}}_{[k|k-1]} - \mathbf{J}\hat{\mathbf{p}}_{[k|k]}\right) \tag{34}$$

$$\mathbf{P}_{\mathrm{x}[k|k]} = \mathbf{P}_{\mathrm{x}[k|k-1]} - \mathbf{K}_{[k]}\left(\tilde{\mathbf{R}}_{[k]} - \mathbf{J}\mathbf{P}_{\mathrm{p}[k|k]}\mathbf{J}^{\mathrm{T}}\right)\mathbf{K}_{[k]}^{\mathrm{T}} \tag{35}$$

$$\mathbf{P}_{\mathrm{xp}[k|k]} = \mathbf{P}_{\mathrm{px}[k|k]}^{\mathrm{T}} = -\mathbf{K}_{[k]}\mathbf{J}\mathbf{P}_{\mathrm{p}[k|k]} \tag{36}$$

Time update

$$\hat{\mathbf{x}}_{[k+1|k]} = \mathbf{A}\hat{\mathbf{x}}_{[k|k]} + \mathbf{B}\hat{\mathbf{p}}_{[k|k]} \tag{37}$$

$$\mathbf{N}_{[k]} = \mathbf{A}\mathbf{K}_{[k]}\left(\mathbf{I}_{n_{\mathrm{d}}} - \mathbf{J}\mathbf{M}_{[k]}\right) + \mathbf{B}\mathbf{M}_{[k]} \tag{38}$$

$$\mathbf{P}_{\mathrm{x}[k+1|k]} = \begin{bmatrix} \mathbf{A} & \mathbf{B} \end{bmatrix} \begin{bmatrix} \mathbf{P}_{\mathrm{x}[k|k]} & \mathbf{P}_{\mathrm{xp}[k|k]} \\ \mathbf{P}_{\mathrm{px}[k|k]} & \mathbf{P}_{\mathrm{p}[k|k]} \end{bmatrix} \begin{bmatrix} \mathbf{A}^{\mathrm{T}} \\ \mathbf{B}^{\mathrm{T}} \end{bmatrix} + \mathbf{Q} - \mathbf{N}_{[k]}\mathbf{S}^{\mathrm{T}} - \mathbf{S}\mathbf{N}_{[k]}^{\mathrm{T}} \tag{39}$$

From the estimated state vector $\hat{\mathbf{x}}_{[k|k]}$ and force vector $\hat{\mathbf{p}}_{[k|k]}$, the response can be estimated at any arbitrary location in the structure, using the following modified output equation:

$$\hat{\mathbf{d}}_{\mathrm{e}[k|k]} = \mathbf{G}_{\mathrm{e}}\hat{\mathbf{x}}_{[k|k]} + \mathbf{J}_{\mathrm{e}}\hat{\mathbf{p}}_{[k|k]} \tag{40}$$

where $\hat{\mathbf{d}}_{\mathrm{e}[k|k]} \in \mathbb{R}^{n_{\mathrm{d_e}}}$ is an estimate of the extrapolated output vector $\mathbf{d}_{\mathrm{e}[k]}$, obtained from the system described by Eqs. (10) and (17). The error covariance matrix corresponding to the output estimate $\hat{\mathbf{d}}_{\mathrm{e}[k|k]}$ is given by:

$$\begin{aligned} \mathbf{P}_{\mathrm{d_e}[k|k]} &\equiv \mathbb{E}\left\{ (\mathbf{d}_{\mathrm{e}[k|k]} - \hat{\mathbf{d}}_{\mathrm{e}[k]})(\mathbf{d}_{\mathrm{e}[k|k]}^{\mathrm{T}} - \hat{\mathbf{d}}_{\mathrm{e}[k]}^{\mathrm{T}}) \right\} \\ &= \mathbf{G}_{\mathrm{e}}\mathbf{P}_{\mathrm{x}[k|k]}\mathbf{G}_{\mathrm{e}}^{\mathrm{T}} + \mathbf{J}_{\mathrm{e}}\mathbf{P}_{\mathrm{p}[k|k]}\mathbf{J}_{\mathrm{e}}^{\mathrm{T}} + \mathbf{G}_{\mathrm{e}}\mathbf{P}_{\mathrm{xp}[k|k]}\mathbf{J}_{\mathrm{e}}^{\mathrm{T}} + \mathbf{J}_{\mathrm{e}}\mathbf{P}_{\mathrm{px}[k|k]}\mathbf{G}_{\mathrm{e}}^{\mathrm{T}} + \mathbf{R}_{\mathrm{e}} \\ &\quad - \mathbf{Z}_{[k]}\mathbf{R}_{\mathrm{c}}^{\mathrm{T}} - \mathbf{R}_{\mathrm{c}}\mathbf{Z}_{[k]}^{\mathrm{T}} \end{aligned} \tag{41}$$

with $\mathbf{Z}_{[k]} = \mathbf{G}_{\mathrm{e}}\mathbf{K}_{[k]}\left(\mathbf{I} - \mathbf{J}\mathbf{M}_{[k]}\right) + \mathbf{J}_{\mathrm{e}}\mathbf{M}_{[k]}$.

In the equations above, the system is assumed to be time-invariant. The algorithm can, however, be readily extended to time-variant systems, by replacing the system matrices $\mathbf{A}$, $\mathbf{B}$, $\mathbf{G}$, $\mathbf{J}$, $\mathbf{G}_{\mathrm{e}}$, and $\mathbf{J}_{\mathrm{e}}$ with the system matrices $\mathbf{A}_{[k]}$, $\mathbf{B}_{[k]}$, $\mathbf{G}_{[k]}$, $\mathbf{J}_{[k]}$, $\mathbf{G}_{\mathrm{e}[k]}$, and $\mathbf{J}_{\mathrm{e}[k]}$, depending on the time step k.

The gain matrices $\mathbf{M}_{[k]}$ and $\mathbf{K}_{[k]}$ are determined such that the input estimates $\hat{\mathbf{p}}_{[k|k]}$ and state estimates $\hat{\mathbf{x}}_{[k|k]}$ are minimum variance and unbiased [2]. The uncertainty on the force and state estimates, quantified by the trace of the error covariance matrices, $\mathrm{tr}(\mathbf{P}_{\mathrm{p}[k|k]})$ and $\mathrm{tr}(\mathbf{P}_{\mathrm{x}[k|k]})$, is minimized, and the error on the estimated forces $\hat{\mathbf{p}}_{[k|k]}$ and states $\hat{\mathbf{x}}_{[k|k]}$ does not depend on the actual forces $\mathbf{p}_{[k]}$. In the presence of modeling errors, the system described by Eqs. (10) and (11) does not represent the true dynamic behavior of the structure. The force and state estimates obtained from the joint input-state estimation algorithm are then no longer minimum variance and unbiased, and the force and state error covariance matrices $\mathbf{P}_{\mathrm{p}[k|k]}$, $\mathbf{P}_{\mathrm{x}[k|k]}$, and $\mathbf{P}_{\mathrm{x}[k+1|k]}$, as defined by Eqs. (32), (35), and (39), respectively, do not correspond to the true error on the biased estimates. Similarly, the expression for the output covariance matrix corresponding to the extrapolated output vector $\mathbf{P}_{\mathrm{d_e}[k|k]}$ in the presence of modeling errors does not correspond to the true error on the biased output estimates. The influence of modeling errors is beyond the scope of this paper, which focuses on estimation errors that originate from additional stochastic excitation and measurement errors.

2.3 Filter transfer functions at steady state

If the conditions for instantaneous system inversion presented in [5] are satisfied, the joint input-state estimation algorithm is stable, and the error covariance matrices $\mathbf{P}_{\mathrm{p}[k|k]}$, $\mathbf{P}_{\mathrm{x}[k|k]}$, $\mathbf{P}_{\mathrm{x}[k|k-1]}$, $\mathbf{P}_{\mathrm{xp}[k|k]}$, and $\mathbf{P}_{\mathrm{px}[k|k]}$ evolve towards a steady state value as

the joint input-state estimation algorithm propagates in time. As a result, the gain matrices $\mathbf{M}_{[k]}$ and $\mathbf{K}_{[k]}$, as well as the matrices $\tilde{\mathbf{R}}_{[k]}$ and $\mathbf{N}_{[k]}$, evolve towards a steady state value. The steady state value of the matrices depends on the noise covariance matrices $\mathbf{Q}$, $\mathbf{R}$, and $\mathbf{S}$, on the forces to be estimated, as well as on the sensor configuration. When the filtering algorithm has reached steady state, the filtering Eqs. (31), (34), and (37) become:

$$\hat{\mathbf{p}}_{[k|k]} = \mathbf{M}^{ss}(\mathbf{d}_{[k]} - \mathbf{G}\hat{\mathbf{x}}_{[k|k-1]}) \tag{42}$$

$$\hat{\mathbf{x}}_{[k|k]} = \hat{\mathbf{x}}_{[k|k-1]} + \mathbf{K}^{ss}(\mathbf{d}_{[k]} - \mathbf{G}\hat{\mathbf{x}}_{[k|k-1]} - \mathbf{J}\hat{\mathbf{p}}_{[k|k]}) \tag{43}$$

$$\hat{\mathbf{x}}_{[k+1|k]} = \mathbf{A}\hat{\mathbf{x}}_{[k|k]} + \mathbf{B}\hat{\mathbf{p}}_{[k|k]} \tag{44}$$

where $\mathbf{M}^{ss}$ and $\mathbf{K}^{ss}$ are the steady state gain matrices obtained from Eqs. (30) and (33), respectively. The matrices are calculated by recursively applying Eqs. (29), (30), and (32) (input estimation), Eqs. (33), (35), and (36) (measurement update), and Eqs. (38) and (39) (time update), until convergence towards a steady state value is observed from the matrix values. Note that the calculation for the steady state gain and error covariance matrices is similar to solving the recursive Riccati differential equation for the steady state value of the state error covariance matrix, in case of the classical Kalman filter [1].

By applying the z-transformation to Eqs. (42) – (44), the following system of equations is obtained:

$$\begin{bmatrix} \mathbf{I}_{n_p} & \mathbf{0} & \mathbf{M}^{ss}\mathbf{G} \\ \mathbf{K}^{ss}\mathbf{J} & \mathbf{I}_{n_s} & -\mathbf{I}_{n_s} + \mathbf{K}^{ss}\mathbf{G} \\ \mathbf{B} & \mathbf{A} & -z\mathbf{I}_{n_s} \end{bmatrix} \begin{bmatrix} \hat{\mathbf{p}}(z) \\ \hat{\mathbf{x}}_0(z) \\ \hat{\mathbf{x}}_1(z) \end{bmatrix} = \begin{bmatrix} \mathbf{M}^{ss} \\ \mathbf{K}^{ss} \\ \mathbf{0} \end{bmatrix} \mathbf{d}(z) \tag{45}$$

where $\hat{\mathbf{p}}(z)$ is the z-transform of $\hat{\mathbf{p}}_{[k|k]}$, $\mathbf{d}(z)$ is the z-transform of $\mathbf{d}_{[k]}$, and $\hat{\mathbf{x}}_m(z)$ is the z-transform of $\hat{\mathbf{x}}_{[k|k-m]}$. Inversion of the system of equations (45) and substituting $z = \exp(i\omega\Delta t)$, directly yield the transfer function matrices that relate the Fourier transform of the estimated force vector $\hat{\mathbf{p}}_{[k|k]}$, denoted by $\hat{\mathbf{p}}(\omega)$, and the Fourier transform of the estimated state vectors $\hat{\mathbf{x}}_{[k|k]}$ and $\hat{\mathbf{x}}_{[k|k-1]}$, denoted by $\hat{\mathbf{x}}_0(\omega)$ and $\hat{\mathbf{x}}_1(\omega)$, respectively, to the Fourier transform of the output vector $\mathbf{d}_{[k]}$, denoted by $\mathbf{d}(\omega)$:

$$\begin{bmatrix} \hat{\mathbf{p}}(\omega) \\ \hat{\mathbf{x}}_0(\omega) \\ \hat{\mathbf{x}}_1(\omega) \end{bmatrix} = \begin{bmatrix} \mathbf{H}_{\hat{p}d}(\omega) \\ \mathbf{H}_{\hat{x}_0 d}(\omega) \\ \mathbf{H}_{\hat{x}_1 d}(\omega) \end{bmatrix} \mathbf{d}(\omega) \tag{46}$$

with

$$\begin{bmatrix} \mathbf{H}_{\hat{p}d}(\omega) \\ \mathbf{H}_{\hat{x}_0 d}(\omega) \\ \mathbf{H}_{\hat{x}_1 d}(\omega) \end{bmatrix} = \begin{bmatrix} \mathbf{I}_{n_p} & \mathbf{0} & \mathbf{M}^{ss}\mathbf{G} \\ \mathbf{K}^{ss}\mathbf{J} & \mathbf{I}_{n_s} & -\mathbf{I}_{n_s} + \mathbf{K}^{ss}\mathbf{G} \\ \mathbf{B} & \mathbf{A} & -\exp(i\omega\Delta t)\mathbf{I}_{n_s} \end{bmatrix}^{-1} \begin{bmatrix} \mathbf{M}^{ss} \\ \mathbf{K}^{ss} \\ \mathbf{0} \end{bmatrix} \tag{47}$$

The transfer function matrix $\mathbf{H}_{\hat{d}_e d}(\omega)$ that relates the Fourier transform of the estimated output vector $\hat{\mathbf{d}}_{e[k|k]}$, denoted by $\hat{\mathbf{d}}_e(\omega)$, to the Fourier transform of the output vector $\mathbf{d}_{[k]}$, is obtained from Eq. (40) by applying the z-transformation and introducing subsequently Eq. (46):

$$\hat{\mathbf{d}}_e(\omega) = \mathbf{H}_{\hat{d}_e d}(\omega)\mathbf{d}(\omega) \tag{48}$$

with

$$\mathbf{H}_{\hat{d}_e d}(\omega) = \mathbf{G}_e \mathbf{H}_{\hat{x}_0 d}(\omega) + \mathbf{J}_e \mathbf{H}_{\hat{p}d}(\omega) \tag{49}$$

2.4 Uncertainty on the estimated quantities

When unknown stochastic excitation and measurement errors are present, and in absence of modeling errors (i.e. $\mathbf{w}_{E[k]} = 0$, $\mathbf{v}_{E[k]} = 0$), introducing Eqs. (12) and (13) into Eqs. (10) and (11), and applying subsequently the z-transformation, yields the following expression for the Fourier transform of the state vector $\mathbf{x}_{[k]}$ and the output vector $\mathbf{d}_{[k]}$:

$$\mathbf{x}(\omega) = \mathbf{H}_{\mathrm{xp}}(\omega)\mathbf{p}(\omega) + \mathbf{H}_{\mathrm{xp_S}}(\omega)\mathbf{p}_S(\omega) \tag{50}$$

$$\mathbf{d}(\omega) = \mathbf{H}_{\mathrm{dp}}(\omega)\mathbf{p}(\omega) + \mathbf{H}_{\mathrm{dp_S}}(\omega)\mathbf{p}_S(\omega) + \mathbf{v}_{\mathrm{M}}(\omega) \tag{51}$$

where $\mathbf{H}_{\mathrm{xp}}(\omega)$ and $\mathbf{H}_{\mathrm{xp_S}}(\omega)$ are the transfer function matrices that relate the Fourier transform of the state vector $\mathbf{x}_{[k]}$, denoted by $\mathbf{x}(\omega)$, to the Fourier transform of the force vector $\mathbf{p}_{[k]}$ and the vector of stochastic forces $\mathbf{p}_{S[k]}$, denoted by $\mathbf{p}(\omega)$ and $\mathbf{p}_S(\omega)$, respectively:

$$\mathbf{H}_{\mathrm{xp}}(\omega) = (\exp(i\omega\Delta t)\mathbf{I}_{n_s} - \mathbf{A})^{-1}\mathbf{B} \tag{52}$$

$$\mathbf{H}_{\mathrm{xp_S}}(\omega) = (\exp(i\omega\Delta t)\mathbf{I}_{n_s} - \mathbf{A})^{-1}\mathbf{B}' \tag{53}$$

The matrices $\mathbf{H}_{\mathrm{dp}}(\omega)$ and $\mathbf{H}_{\mathrm{dp_S}}(\omega)$ are the transfer function matrices that relate the Fourier transform of the output vector $\mathbf{d}_{[k]}$, denoted by $\mathbf{d}(\omega)$, to the Fourier transform of the force vector $\mathbf{p}_{[k]}$ and the vector of stochastic forces $\mathbf{p}_{S[k]}$, respectively:

$$\mathbf{H}_{\mathrm{dp}}(\omega) = \mathbf{G}\mathbf{H}_{\mathrm{xp}}(\omega) + \mathbf{J} \tag{54}$$

$$\mathbf{H}_{\mathrm{dp_S}}(\omega) = \mathbf{G}\mathbf{H}_{\mathrm{xp_S}}(\omega) + \mathbf{J}' \tag{55}$$

Introducing Eq. (18) into Eq. (16) and applying subsequently the z-transformation, yields the following expression for the Fourier transform of the output vector $\mathbf{d}_{\mathrm{e}[k]}$ corresponding to the extrapolated output quantities:

$$\mathbf{d}_{\mathrm{e}}(\omega) = \mathbf{H}_{\mathrm{d_ep}}(\omega)\mathbf{p}(\omega) + \mathbf{H}_{\mathrm{d_ep_S}}(\omega)\mathbf{p}_S(\omega) \tag{56}$$

where $\mathbf{H}_{\mathrm{d_ep}}(\omega)$ and $\mathbf{H}_{\mathrm{d_ep_S}}(\omega)$ are the transfer function matrices that relate the Fourier transform of the output vector $\mathbf{d}_{\mathrm{e}[k]}$, denoted by $\mathbf{d}_{\mathrm{e}}(\omega)$, to the Fourier transform of the force vector $\mathbf{p}_{[k]}$ and the vector of stochastic forces $\mathbf{p}_{S[k]}$, respectively:

$$\mathbf{H}_{\mathrm{d_ep}}(\omega) = \mathbf{G}_{\mathrm{e}}\mathbf{H}_{\mathrm{xp}}(\omega) + \mathbf{J}_{\mathrm{e}} \tag{57}$$

$$\mathbf{H}_{\mathrm{d_ep_S}}(\omega) = \mathbf{G}_{\mathrm{e}}\mathbf{H}_{\mathrm{xp_S}}(\omega) + \mathbf{J}_{\mathrm{e}}' \tag{58}$$

Introducing Eq. (51) in Eq. (46) yields the error on the Fourier transform of the estimated force vector $\hat{\mathbf{p}}_{[k|k]}$:

$$\tilde{\mathbf{p}}(\omega) \equiv \mathbf{p}(\omega) - \hat{\mathbf{p}}(\omega)$$
$$= (\mathbf{I}_{n_p} - \mathbf{H}_{\hat{\mathbf{p}}\mathrm{d}}(\omega)\mathbf{H}_{\mathrm{dp}}(\omega))\mathbf{p}(\omega) - \mathbf{H}_{\hat{\mathbf{p}}\mathrm{d}}(\omega)\mathbf{H}_{\mathrm{dp_S}}(\omega)\mathbf{p}_S(\omega) - \mathbf{H}_{\hat{\mathbf{p}}\mathrm{d}}(\omega)\mathbf{v}_{\mathrm{M}}(\omega) \tag{59}$$

Introducing Eq. (51) in Eq. (46), and taking into account Eq. (50), yields the error on the Fourier transform of the estimated state vector $\hat{\mathbf{x}}_{[k|k-m]}$:

$$\tilde{\mathbf{x}}_m(\omega) \equiv \mathbf{x}(\omega) - \hat{\mathbf{x}}_m(\omega)$$
$$= (\mathbf{H}_{\mathrm{xp}}(\omega) - \mathbf{H}_{\hat{\mathbf{x}}_m\mathrm{d}}(\omega)\mathbf{H}_{\mathrm{dp}}(\omega))\mathbf{p}(\omega) + (\mathbf{H}_{\mathrm{xp_S}}(\omega) - \mathbf{H}_{\hat{\mathbf{x}}_m\mathrm{d}}(\omega)\mathbf{H}_{\mathrm{dp_S}}(\omega))\mathbf{p}_S(\omega)$$
$$- \mathbf{H}_{\hat{\mathbf{x}}_m\mathrm{d}}(\omega)\mathbf{v}_{\mathrm{M}}(\omega) \tag{60}$$

Introducing Eq. (51) in Eq. (48), and taking into account Eq. (56), yields the error on the Fourier transform of the estimated output vector $\hat{\mathbf{d}}_{\mathrm{e}[k|k]}$:

$$
\begin{aligned}
\tilde{\mathbf{d}}_{\mathrm{e}}(\omega) &\equiv \mathbf{d}_{\mathrm{e}}(\omega) - \hat{\mathbf{d}}_{\mathrm{e}}(\omega) \\
&= (\mathbf{H}_{\mathrm{d_e p}}(\omega) - \mathbf{H}_{\hat{\mathrm{d}}_{\mathrm{e}}\mathrm{d}}(\omega)\mathbf{H}_{\mathrm{dp}}(\omega))\mathbf{p}(\omega) + (\mathbf{H}_{\mathrm{d_e p_S}}(\omega) - \mathbf{H}_{\hat{\mathrm{d}}_{\mathrm{e}}\mathrm{d}}(\omega)\mathbf{H}_{\mathrm{dp_S}}(\omega))\mathbf{p}_{\mathrm{S}}(\omega) \\
&\quad - \mathbf{H}_{\hat{\mathrm{d}}_{\mathrm{e}}\mathrm{d}}(\omega)\mathbf{v}_{\mathrm{M}}(\omega)
\end{aligned}
\tag{61}
$$

Eqs. (59) – (61) show that the errors on the estimated quantities consist of three components. The first term in the right hand side of Eqs. (59) – (61) is due to modeling errors. In absence of modeling errors, this term equals zero and therefore vanishes. The second and third term in the right hand side of Eqs. (59) – (61) are due to additional stochastic excitation and measurement errors, respectively. In the following, the focus will go to the errors that originate from additional stochastic excitation and measurement errors.

In absence of modeling errors, and assuming the stochastic forces $\mathbf{p}_{\mathrm{S}[k]}$ and the measurement errors $\mathbf{v}_{\mathrm{M}[k]}$ to be stationary and mutually uncorrelated (i.e. $\mathbb{E}\{\mathbf{p}_{\mathrm{S}[k]}\mathbf{v}_{\mathrm{M}[l]}\} = \mathbf{0}$), the PSD function of the error on the estimated force vector $\tilde{\mathbf{p}}_{[k|k]}$ ($\equiv \mathbf{p}_{[k]} - \hat{\mathbf{p}}_{[k|k]}$) is directly obtained from Eq. (59):

$$
\mathbf{S}_{\tilde{\mathbf{p}}\tilde{\mathbf{p}}}(\omega) = \mathbf{H}_{\hat{\mathrm{p}}\mathrm{d}}(\omega)\mathbf{H}_{\mathrm{dp_S}}(\omega)\mathbf{S}_{\mathrm{P_S P_S}}(\omega)\mathbf{H}_{\mathrm{dp_S}}^{*}(\omega)\mathbf{H}_{\hat{\mathrm{p}}\mathrm{d}}^{*}(\omega) + \mathbf{H}_{\hat{\mathrm{p}}\mathrm{d}}(\omega)\mathbf{S}_{\mathrm{v_M v_M}}(\omega)\mathbf{H}_{\hat{\mathrm{p}}\mathrm{d}}^{*}(\omega)
\tag{62}
$$

where $\square^{*}$ denotes the Hermitian transpose of a matrix. The AC function of the error is obtained as the inverse Fourier transform of the PSD function (Eq. (19)). The PSD function and AC function of the error on the estimated state vector $\tilde{\mathbf{x}}_{[k|k-m]}$ ($\equiv \mathbf{x}_{[k]} - \hat{\mathbf{x}}_{[k|k-m]}$) and the error on the estimated extrapolated output vector $\tilde{\mathbf{d}}_{\mathrm{e}[k|k]}$ ($\equiv \mathbf{d}_{\mathrm{e}[k]} - \hat{\mathbf{d}}_{\mathrm{e}[k|k]}$) are obtained similarly from Eqs. (60) and (61), respectively. The PSD function of the errors is given by the following expressions:

$$
\begin{aligned}
\mathbf{S}_{\tilde{\mathbf{x}}_m\tilde{\mathbf{x}}_m}(\omega) = {}&(\mathbf{H}_{\mathrm{xp_S}}(\omega) - \mathbf{H}_{\hat{\mathrm{x}}_m\mathrm{d}}(\omega)\mathbf{H}_{\mathrm{dp_S}}(\omega))\mathbf{S}_{\mathrm{P_S P_S}}(\omega)(\mathbf{H}_{\mathrm{xp_S}}^{*}(\omega) - \mathbf{H}_{\mathrm{dp_S}}^{*}(\omega)\mathbf{H}_{\hat{\mathrm{x}}_m\mathrm{d}}^{*}(\omega)) \\
&+ \mathbf{H}_{\hat{\mathrm{x}}_m\mathrm{d}}(\omega)\mathbf{S}_{\mathrm{v_M v_M}}(\omega)\mathbf{H}_{\hat{\mathrm{x}}_m\mathrm{d}}^{*}(\omega)
\end{aligned}
\tag{63}
$$

$$
\begin{aligned}
\mathbf{S}_{\tilde{\mathbf{d}}_e\tilde{\mathbf{d}}_e}(\omega) = {}&(\mathbf{H}_{\mathrm{d_e p_S}}(\omega) - \mathbf{H}_{\hat{\mathrm{d}}_{\mathrm{e}}\mathrm{d}}(\omega)\mathbf{H}_{\mathrm{dp_S}}(\omega))\mathbf{S}_{\mathrm{P_S P_S}}(\omega)(\mathbf{H}_{\mathrm{d_e p_S}}^{*}(\omega) - \mathbf{H}_{\mathrm{dp_S}}^{*}(\omega)\mathbf{H}_{\hat{\mathrm{d}}_{\mathrm{e}}\mathrm{d}}^{*}(\omega)) \\
&+ \mathbf{H}_{\hat{\mathrm{d}}_{\mathrm{e}}\mathrm{d}}(\omega)\mathbf{S}_{\mathrm{v_M v_M}}(\omega)\mathbf{H}_{\hat{\mathrm{d}}_{\mathrm{e}}\mathrm{d}}^{*}(\omega)
\end{aligned}
\tag{64}
$$

In the case where the additional stochastic excitation and the measurement errors meet the white noise assumption, and if the covariance matrices $\mathbf{C}_{\mathrm{p}}$ and $\mathbf{R}_{\mathrm{M}}$, defined in Eqs. (21) and (23), respectively, are known, the covariance matrices $\mathbf{Q}$, $\mathbf{R}$, and $\mathbf{S}$ characterizing the actual process noise $\mathbf{w}_{[k]}$ and measurement noise $\mathbf{v}_{[k]}$ are obtained from the following equation:

$$
\begin{bmatrix} \mathbf{Q} & \mathbf{S} \\ \mathbf{S}^{\mathrm{T}} & \mathbf{R} \end{bmatrix} = \begin{bmatrix} \mathbf{B}' \\ \mathbf{J}' \end{bmatrix} \mathbf{C}_{\mathrm{p}} \begin{bmatrix} \mathbf{B}'^{\mathrm{T}} & \mathbf{J}'^{\mathrm{T}} \end{bmatrix} + \begin{bmatrix} \mathbf{0} & \mathbf{0} \\ \mathbf{0} & \mathbf{R}_{\mathrm{M}} \end{bmatrix}
\tag{65}
$$

Applying the matrices $\mathbf{Q}$, $\mathbf{R}$, and $\mathbf{S}$ obtained from Eq. (65) for joint input-state estimation in this case yields minimum variance and unbiased errors on the estimates of the forces and system states. The AC of the error on the estimated force vector $\tilde{\mathbf{p}}_{[k|k]}$ and

state vector $\tilde{\mathbf{x}}_{[k|k-m]}$, for a time lag $l = 0$ by definition equals the corresponding steady state error covariance matrix obtained from the joint input-state estimation algorithm:

$$\mathbf{R}_{\tilde{p}\tilde{p}[0]} = \mathbf{P}_{\mathrm{p}}^{\mathrm{ss}} \text{ and } \mathbf{R}_{\tilde{x}_m\tilde{x}_m[0]} = \mathbf{P}_{\mathrm{x}m}^{\mathrm{ss}} \tag{66}$$

where $\mathbf{P}_{\mathrm{p}}^{\mathrm{ss}}$ and $\mathbf{P}_{\mathrm{x}m}^{\mathrm{ss}}$ are the steady state error covariance matrices $\mathbf{P}_{\mathrm{p}[k|k]}$, $\mathbf{P}_{\mathrm{x}[k|k]}$ ($m = 0$), and $\mathbf{P}_{\mathrm{x}[k|k-1]}$ ($m = 1$), obtained from Eqs. (32), (35), and (39), respectively. The covariance matrices $\mathbf{R}_{\mathrm{e}}$ and $\mathbf{R}_{\mathrm{c}}$, characterizing the actual measurement noise $\mathbf{v}_{\mathrm{e}[k]}$, are obtained from the following equation:

$$\begin{bmatrix} \mathbf{R}_{\mathrm{e}} & \mathbf{R}_{\mathrm{c}} \end{bmatrix} = \mathbf{J}_{\mathrm{e}}' \mathbf{C}_{\mathrm{p}} \begin{bmatrix} \mathbf{J}_{\mathrm{e}}'^{\mathrm{T}} & \mathbf{J}'^{\mathrm{T}} \end{bmatrix} \tag{67}$$

The AC of the error on the estimated extrapolated output vector $\tilde{\mathbf{d}}_{\mathrm{e}[k|k]}$ for a time lag $l = 0$ by definition equals the corresponding steady state error covariance matrix $\mathbf{P}_{\mathrm{d}_{\mathrm{e}}[k|k]}$ obtained from Eq. (41), applying the matrices $\mathbf{R}_{\mathrm{e}}$ and $\mathbf{R}_{\mathrm{c}}$ obtained from Eq. (67):

$$\mathbf{R}_{\tilde{d}_{\mathrm{e}}\tilde{d}_{\mathrm{e}}[0]} = \mathbf{P}_{\mathrm{d}_{\mathrm{e}}}^{\mathrm{ss}} \tag{68}$$

where $\mathbf{P}_{\mathrm{d}_{\mathrm{e}}}^{\mathrm{ss}}$ is the steady state error covariance matrix, obtained from Eq. (41).

If the noise covariance matrices $\mathbf{Q}$, $\mathbf{R}$, and $\mathbf{S}$ assumed for joint input-state estimation do not correspond to the true covariance of the white noise processes, or if the true noise processes do not meet the white assumption, the errors on the force, state, and response estimates obtained from the joint input-state estimation algorithm are not minimum variance. In addition, the error covariance matrices $\mathbf{P}_{\mathrm{p}[k|k]}$, $\mathbf{P}_{\mathrm{x}[k|k-m]}$, and $\mathbf{P}_{\mathrm{d}_{\mathrm{e}}[k|k]}$ do no longer give the covariance of the error on the estimated quantities. Eqs. (59) – (61) remain valid, however, so that the PSD function of the actual error on the estimated quantities is still obtained from Eqs. (62) – (64).

The approach for quantification of the estimation uncertainty presented in this section, for the case of joint input-state estimation, can be extended to other force and state estimation algorithms. This extension is performed by replacing the filter transfer functions presented in Section 2.3 with the transfer functions of the force or state estimation algorithm under consideration.

3   VERIFICATION EXAMPLE

The uncertainty quantification procedure is illustrated and verified using numerical simulations. The structure under consideration is the cantilever steel beam shown in Figure 1. The beam has a rectangular cross section with a width of 50.8 mm and a height of 25.4 mm. The beam has a length of 1 m. The Young's modulus and material density are taken as 210 GPa and 7750 kg/m^3, respectively.
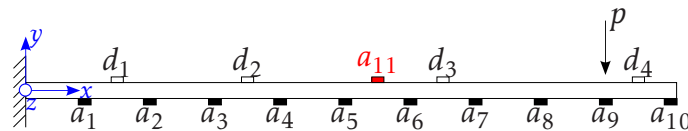

Figure 1: Side view cantilever beam, force and sensor configuration (p: force, a_i: accelerometer i, and d_i: displacement sensor i).

The beam is modeled using 100 2D finite element (FE) Euler-Bernoulli beam elements. Only bending in the vertical plane is considered. The first four natural frequencies obtained from the beam model are 21.4 Hz, 133.7 Hz, 374.0 Hz, and 731.6 Hz.

The corresponding bending mode shapes in the vertical plane are shown in Figure 2. A modal damping ratio of 2.5% is assumed for the four modes.
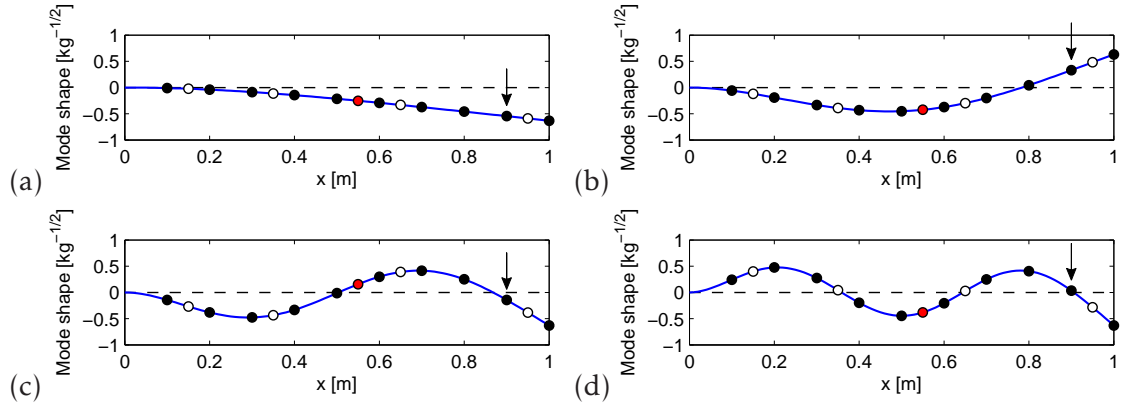

Figure 2: Mass normalized mode shape along the neutral axis of the beam, for (a) mode 1, (b) mode 2, (c) mode 3, and (d) mode 4. The undeformed neutral axis is shown by a black dashed line. The markers indicate the sensor positions (marker colors: see Figure 1). The arrow indicates the force location.

3.1   System model

A discrete-time modally reduced order state-space model is constructed from the first four bending modes of the beam. A zero order hold assumption on the input vector $\mathbf{p}_{[k]}$ is applied in the discretization of the system, using a sampling rate of 4 kHz. The state-feedback matrix $\mathbf{A}$ and the state-input matrix $\mathbf{B}$ are calculated from Eqs. (4) and (5). The state-output matrix $\mathbf{G}$ and the direct transmission matrix $\mathbf{J}$ are calculated from Eqs. (8) and (9).

In the following analysis, the response vector $\mathbf{d}_{[k]}$ includes a subset of ten vertical accelerations, $a_1 - a_{10}$, and four vertical displacements, $d_1 - d_4$. The input $\mathbf{p}_{[k]}$, to be estimated, consists of one vertical force p, applied at a distance of 0.1 m from the free end of the beam. The output $\mathbf{d}_{e[k]}$, to be estimated, consists of one vertical acceleration, a_{11}. The locations of the specified inputs and outputs are shown in Figure 1.

3.2   Joint input-state estimation

The joint input-state estimation algorithm introduced in Section 2.2 is first applied for the identification of an impact force and the estimation of the corresponding extrapolated response, in the absence of measurement errors and additional stochastic excitation. The impact force is a triangular pulse that increases linearly from zero at time $t = 0.2$ s to 100 N at $t = 0.202$ s, before decreasing linearly to zero at $t = 0.204$ s. From the conditions for instantaneous system inversion derived in [5], it is found that the output vector $\mathbf{d}_{[k]}$ should contain at least one acceleration and one displacement measurement. By including an acceleration measurement, direct feedthrough from the system input $\mathbf{p}_{[k]}$ to the output $\mathbf{d}_{[k]}$ is ensured through the matrix $\mathbf{J}$ in Eq. (9). This direct feedthrough is necessary for instantaneous system inversion, i.e. inversion without any time delay. The displacement is required in order to obtain a stable system inverse with a unique solution (see also [5]). The system response $\mathbf{d}_{[k]}$ in this case consists of one acceleration a_9 and one displacement d_4, see also Figure 1. The response

is obtained from a forward time domain calculation, hereby applying the impact force time history $\mathbf{p}_{[k]}$ as input to the state-space model given by Eqs. (10) and (11).

The initial state vector $\hat{\mathbf{x}}_{[0|-1]}$ and its corresponding error covariance matrix $\mathbf{P}_{\mathrm{x}[0|-1]}$ are both assigned a zero value for the application of the joint input-state estimation algorithm. No additional stochastic excitation is present. The noise covariance matrices $\mathbf{Q}$ and $\mathbf{S}$ are therefore assumed zero. Although no additional stochastic excitation and measurement errors are present, the matrix $\mathbf{R}$ must be positive definite, and can therefore not be assigned a zero value (see also Section 2.2). A standard deviation $\sigma_{\mathrm{M,a}} = 10^{-2}$ m/s² and $\sigma_{\mathrm{M,d}} = 10^{-6}$ m is assumed for the measurement error on the acceleration and displacement signals, respectively. This choice, however, does not affect the results obtained in this section.

Figure 3 compares the estimated force obtained from joint input-state estimation to the applied impact force. Figure 4 compares the estimated acceleration $\hat{a}_{11}$ to the corresponding actual acceleration, obtained from a forward time domain calculation. The estimated force and extrapolated response perfectly agree with the true force and response, respectively. This illustrates that, in the absence of additional stochastic excitation and measurement errors, the algorithm is able to perfectly reconstruct the actual forces and system states, which can be used to extrapolate the response to any location in the structure.
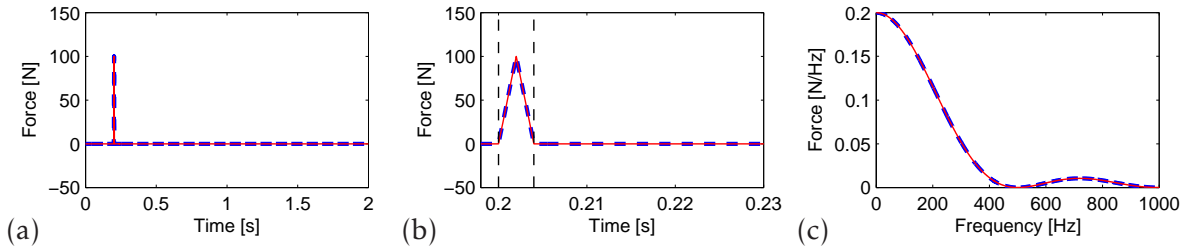
Figure 3: (a) Time history, (b) detail time history, and (c) amplitude of the narrow band frequency spectrum of the applied impact force (blue dashed line) and the estimated force (red solid line). The begin and end of the impact are indicated in (b) by a vertical dashed line.
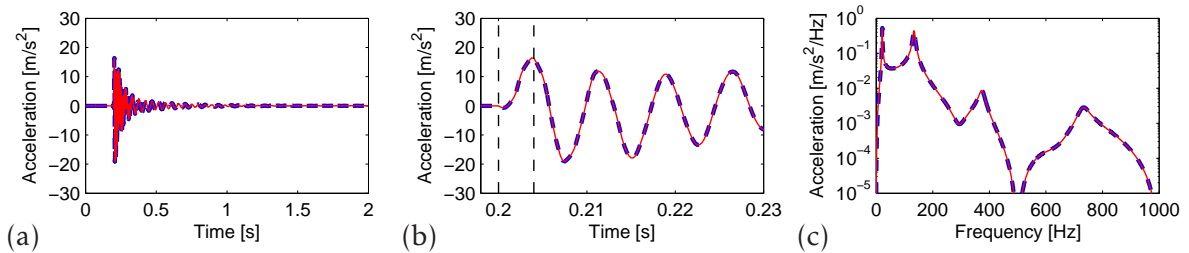

Figure 4: (a) Time history, (b) detail time history, and (c) amplitude of the narrow band frequency spectrum of the actual acceleration a_{11} (blue dashed line) and the estimated acceleration (red solid line). The begin and end of the impact are indicated in (b) by a vertical dashed line.

3.3 Filter transfer functions at steady state

The transfer functions of the joint input-state estimation algorithm at steady state, derived in Section 2.3, relate the estimated quantities to the measured data. The transfer functions can be used to quantify the uncertainty on the results obtained from

joint input-state estimation, that is introduced by additional stochastic excitation and measurement errors, as will be illustrated in Section 3.4. Apart from their use in the quantification of the errors, the transfer functions also yield insight into the way the algorithm weighs the available response data, as illustrated in this section.

Figure 5 shows the transfer functions $H_{\hat{p}d}(\omega)$ that relate the Fourier transform of the estimated force $\hat{p}$ to the Fourier transform of acceleration a_9 and displacement d_4 (note: for notational convenience, the elements of a matrix $\mathbf{X}$ are indicated by X throughout the entire paper). The transfer function $H_{\hat{p}d}(\omega)$ has been calculated for the sensor configuration assumed for joint input-state estimation in Section 3.2. The noise covariance matrices $\mathbf{Q}$ and $\mathbf{S}$ are assumed zero, i.e. no stochastic excitation present. For the measurement errors and so the noise covariance matrix $\mathbf{R}$, two different cases are considered. For the first case, the noise statistics are assumed identical to the ones assumed in Section 3.2, i.e. $\sigma_{M,a} = 10^{-2}$ m/s^2 and $\sigma_{M,d} = 10^{-6}$ m. For the second case, a lower measurement uncertainty is assumed for the displacement measurement, using a standard deviation $\sigma_{M,d} = 10^{-7}$ m for the measurement error on the displacement signal. The measurement uncertainty for the acceleration measurement is assumed identical to the first case, i.e. $\sigma_{M,a} = 10^{-2}$ m/s^2. The transfer function $H_{\hat{p}d}(\omega)$ that relates the Fourier transform of the estimated force $\hat{p}$ to the Fourier transform of acceleration a_9 (Figure 5a) in both cases is characterized by a dip at the second, third, and fourth natural frequency, and a peak at the antiresonance frequencies of the transfer function $H_{dp}(\omega)$ that relates the Fourier transform of the output vector $\mathbf{d}_{[k]}$ to the Fourier transform of the force vector $\mathbf{p}_{[k]}$. For frequencies lower than the second natural frequency, the transfer function $H_{\hat{p}d}(\omega)$ strongly depends on the standard deviation $\sigma_{M,d}$ assumed in the calculation of the transfer function. This variation with the standard deviation $\sigma_{M,d}$ is related to the way the algorithm weighs the acceleration and displacement data, as explained next. The transfer function $H_{\hat{p}d}(\omega)$ that relates the Fourier transform of the estimated force $\hat{p}$ to the Fourier transform of the displacement d_4 (Figure 5b) strongly depends on the measurement uncertainty on the displacement measurement assumed. For the first case ($\sigma_{M,d} = 10^{-6}$ m), the transfer function $H_{\hat{p}d}(\omega)$ is not characterized by any clear dips or peaks. For the second case, which corresponds to a lower measurement uncertainty for the displacement measurement ($\sigma_{M,d} = 10^{-7}$ m), the transfer function $H_{\hat{p}d}(\omega)$ for most frequencies differs one order of magnitude from the transfer function in the first case and shows some clear peaks and dips that depend on the natural frequencies and the antiresonance frequencies of the transfer function $H_{dp}(\omega)$. This can be explained as follows. For each frequency ω, the joint input-state estimation algorithm weighs the displacement and acceleration data in the estimation of the forces and system states, such that the errors on the estimated forces and system states are minimum variance. The weighing is based on the process and measurement noise covariance matrices, $\mathbf{Q}$, $\mathbf{R}$, and $\mathbf{S}$. At low frequencies, the information is mostly contained in the displacement data, whereas at higher frequencies the displacement data in case of large measurement uncertainty becomes non-informative due to measurement noise. The absence of clear peaks and dips in the transfer function $H_{\hat{p}d}(\omega)$ that relates the Fourier transform of the estimated force $\hat{p}$ to the Fourier transform of the displacement d_4 for the first case therefore indicates that the displacement data only contribute to the estimated force at very low frequencies. The value of the transfer function $H_{\hat{p}d}(\omega)$ that relates the Fourier transform of the estimated force $\hat{p}$ to the Fourier transform of the displacement d_4 at 0 Hz is equal to 5.53×10^4 N/m. This

value does not depend on the noise statistics assumed for joint input-state estimation, and perfectly corresponds to the static stiffness of the beam.
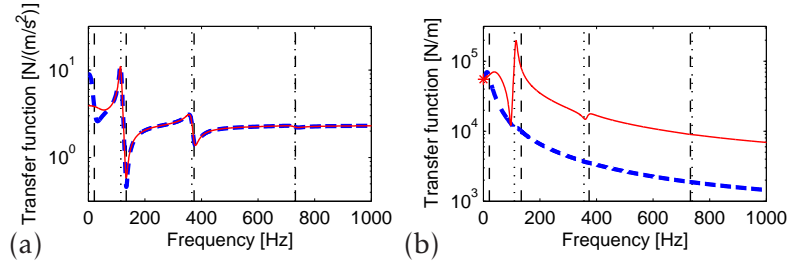

(a)   (b)

Figure 5: Amplitude of the transfer function $H_{\hat{p}d}(\omega)$ that relates the Fourier transform of the estimated force $\hat{p}$ to the Fourier transform of (a) acceleration a_9 and (b) displacement d_4, for case 1 ($\sigma_{M,d} = 10^{-6}$ m, blue dashed line) and case 2 ($\sigma_{M,d} = 10^{-7}$ m, red solid line). The undamped natural frequencies are indicated by vertical dashed lines. The antiresonance frequencies of the transfer functions $H_{dp}(\omega)$ that relate the Fourier transform of (a) acceleration a_9 and (b) displacement d_4 to the Fourier transform of the force p are indicated by vertical dotted lines.

Figure 6 shows the transfer functions $H_{\hat{d}_e d}(\omega)$ that relate the Fourier transform of the estimated acceleration $\hat{a}_{11}$ to the Fourier transform of acceleration a_9 and displacement d_4. For the measurement uncertainty on the response data, the two cases introduced in the previous paragraph are considered. The transfer functions $H_{\hat{d}_e d}(\omega)$ depend on the relation of the output $\mathbf{d}_{[k]}$ to the input p, as described by the transfer functions $H_{dp}(\omega)$, on the relation of the output $\mathbf{d}_{e[k]}$ to the input p, as described by the transfer functions $H_{d_e p}(\omega)$, and on the noise covariance matrices, $\mathbf{Q}$, $\mathbf{R}$, and $\mathbf{S}$, that determine the weighing of the data in the estimation. The transfer function $H_{\hat{d}_e d}(\omega)$ that relates the Fourier transform of the estimated acceleration $\hat{a}_{11}$ to the Fourier transform of acceleration a_9 (Figure 6a) does not show a clear variation with the standard deviation $\sigma_{M,d}$ assumed. The transfer function $H_{\hat{d}_e d}(\omega)$ that relates the Fourier transform of the estimated acceleration $\hat{a}_{11}$ to the Fourier transform of displacement d_4 (Figure 6b), on the other hand, shows a clear variation with the standard deviation $\sigma_{M,d}$ over the entire frequency range of interest. In addition, this transfer function for both values of $\sigma_{M,d}$ is characterized by peaks and dips. The four modes included in the system model cannot be distinguished from a single acceleration measurement. Taking into account the displacement in the estimation of the system states will lead to a decreased uncertainty on the estimated (modal) states and, therefore, on the estimated extrapolated response. The presence of clear peaks and dips in the transfer function that relates the Fourier transform of the estimated acceleration $\hat{a}_{11}$ to the Fourier transform of the displacement d_4 indicates that the displacement data contribute to the estimated acceleration $\hat{a}_{11}$ for the entire frequency range of interest.

3.4 Error on the estimated quantities

This section illustrates how the error covariance matrices obtained from the joint input-state estimation algorithm (Section 2.2) or, more generally, the AC and PSD functions of the errors, directly obtained from the filter transfer functions (Section 2.3), can be used to quantify the uncertainty on the estimation results. Two cases are considered, corresponding to different types of additional stochastic excitation: the first case considers white noise stochastic excitation, the second case considers colored noise
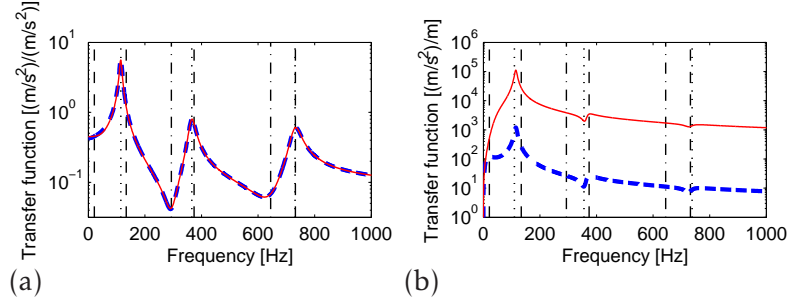
Figure 6: Amplitude of the transfer function $H_{\hat{\mathbf{d}}_e \mathbf{d}}(\omega)$ that relates the Fourier transform of the estimated acceleration $\hat{a}_{11}$ to the Fourier transform of (a) acceleration a_9 and (b) displacement d_4, for case 1 ($\sigma_{\mathrm{M,d}} = 10^{-6}$ m, blue dashed line) and case 2 ($\sigma_{\mathrm{M,d}} = 10^{-7}$ m, red solid line). The undamped natural frequencies are indicated by vertical dashed lines. The antiresonance frequencies of the transfer functions $H_{\mathrm{dp}}(\omega)$ that relate the Fourier transform of (a) acceleration a_9 and (b) displacement d_4 to the Fourier transform of the force p are indicated by vertical dotted lines. The antiresonance frequencies of the transfer function $H_{\mathbf{d}_e \mathbf{p}}(\omega)$ that relates the Fourier transform acceleration a_{11} to the Fourier transform of the force p are indicated by vertical dash-dotted lines.

stochastic excitation. In the first case, all assumptions made for the derivation of the joint input-state estimation algorithm are met. In the second case, the white noise assumption is violated.

It follows immediately from Eqs. (59), (60), and (61) that the errors on the estimated quantities introduced by measurement errors and additional stochastic excitation are independent of the actual force $\mathbf{p}_{[k]}$, which is therefore assumed zero in the following analysis. The data $\mathbf{d}_{[k]}$ passed to the joint input-state estimation algorithm consists of acceleration a_9 and displacement d_4, and is obtained from Eqs. (10) – (15), for $\mathbf{p}_{[k]} = \mathbf{0}$. The error on the estimated response vector $\hat{\mathbf{d}}_{e[k|k]}$, which consists of acceleration $\hat{a}_{11}$, is calculated as $\tilde{\mathbf{d}}_{e[k|k]} = \mathbf{d}_{e[k]} - \hat{\mathbf{d}}_{e[k|k]}$, where the response vector $\mathbf{d}_{e[k]}$ obtained from Eqs. (10), (17), and (18), for $\mathbf{p}_{[k]} = \mathbf{0}$. A sampling period $T = 500$ s is assumed in the analysis.

Ten uncorrelated vertical stochastic forces are considered, acting at the locations of accelerometers $a_1 - a_{10}$ (see Figure 1). For the case where white noise stochastic excitation is considered, the stochastic forces are drawn independently from a normal distribution with zero mean value and a standard deviation σ_{p_S} of 0.1 N. For the cases where colored noise stochastic excitation is considered, the Fourier transform of the jth stochastic force ($j = 1, \ldots, 10$) is calculated for $N/2$ discrete frequencies ω_n ($= 2\pi(n-1)/(N\Delta t)$; $n = 1, \ldots, N/2$) from the following equation:

$$\mathbf{p}_{Sj}(\omega_n) = \exp(i\phi_n)\sqrt{N\Delta t \mathbf{S}_{p_{Sj}p_{Sj}}(\omega_n)} \tag{69}$$

with $\mathbf{S}_{p_{Sj}p_{Sj}}(\omega)$ the PSD function of the stationary stochastic force, for component j, N the number of time steps in the simulation, and Δt the sampling time step. The phase angle ϕ_n is drawn independently from a uniform distribution over the interval $[0, 2\pi]$, see also [12]. The time history $\mathbf{p}_{Sj[k]}$ is subsequently obtained from the (discrete) inverse Fourier transform of $\mathbf{p}_{Sj}(\omega_n)$. The PSD function of the stationary stochastic forces $\mathbf{S}_{p_{Sj}p_{Sj}}(\omega)$ is assumed identical for the n_{p_S} components, and is given by:

$$\mathbf{S}_{p_{Sj}p_{Sj}}(\omega) = \frac{\omega}{(1+\omega)^2} \tag{70}$$

Figure 7 shows the PSD function of the stochastic forces and its corresponding AC function. The AC function shows a clear correlation of the stochastic forces over time, whereas the PSD function shows that the stochastic forces are mainly dominated by low frequency components.
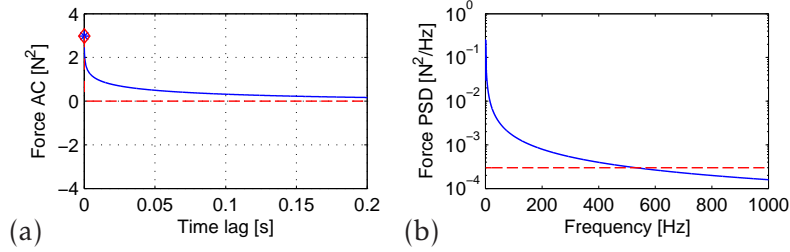

Figure 7: (a) AC function and (b) PSD function of the stochastic forces applied in the simulations (blue solid line) and comparison to the equivalent white noise assumed for joint input-state estimation (red dashed line).

The measurement errors $\mathbf{v}_{M[k]}$ are drawn independently from a normal distribution with zero mean value and a standard deviation of 10^{-6} m and 10^{-2} m/s^2 for the displacement and acceleration measurements, respectively.

The noise covariance matrices $\mathbf{Q}$, $\mathbf{R}$, and $\mathbf{S}$, assumed for joint input-state estimation, are calculated from Eq. (65). Note that the joint input-state estimation algorithm assumes white process and measurement noise, i.e. a flat PSD function over the entire frequency range for both the measurement errors and stochastic forces. For colored noise stochastic forces, however, the white noise assumption is not satisfied. Equivalent white noise with stochastic force covariance matrix $\mathbf{C}_\mathrm{p} = \mathbf{R}_{\mathrm{p_S p_S}}[0]$ is assumed. Figure 7 compares the true noise AC and PSD function to the ones of the equivalent white noise. Another choice of the matrix $\mathbf{C}_\mathrm{p}$ will lead to different errors on the estimated quantities.

White noise stochastic excitation Figure 8 shows the evolution of the error variance of the estimated force $\hat{p}$ and the estimated acceleration $\hat{a}_{11}$ with time. The variances are found as the diagonal values of the error covariance matrices $\mathbf{P}_{\mathrm{p}[k|k]}$ and $\mathbf{P}_{\mathrm{d_e}[k|k]}$, obtained from the joint input-state estimation algorithm. The error variance for both estimated quantities evolves over time towards a steady state value. For both estimated quantities only a very a short time period is required to reach steady state. This justifies the steady state assumption made in sections 2.3 and 2.4 for the calculation of the filter transfer functions and the quantification of the errors on the results obtained.

Figures 9 and 10 show the time history, the sample AC and PSD function of the error on the estimated force $\hat{p}$ and the estimated acceleration $\hat{a}_{11}$, respectively, as obtained from the numerical simulations. The sample PSD function is estimated using Welch's method, hereby applying a window length of 2048 samples and an overlap of 66%. The sample AC function of the error on both estimated quantities shows a significant correlation with time, resulting in a non-flat PSD function. The sample PSD function of the errors shows a peak at the antiresonance frequencies of the transfer functions $H_{\mathrm{dp}}(\omega)$. This indicates that the estimation errors depend on the zeros of the transfer functions $H_{\mathrm{dp}}(\omega)$. Unstable zeros lead to large errors on the estimated quantities, due to the amplification of measurement errors and, therefore, should be avoided.
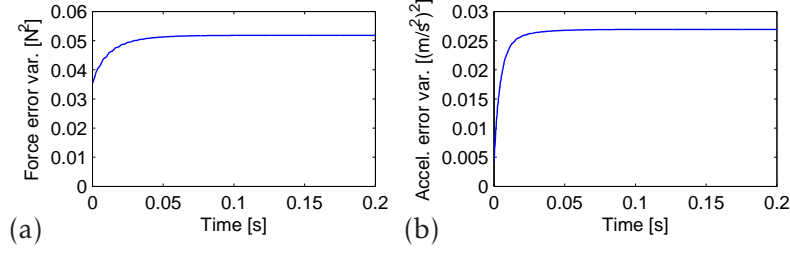
Figure 8: Evolution of the error variance of (a) the estimated force $\hat{p}$ and (b) the estimated acceleration $\hat{a}_{11}$, for white noise stochastic excitation.

Figures 9 and 10 also compare the sample AC and PSD function of the error on the estimated quantities to the AC and PSD obtained from Eqs. (19), (62), and (64). The comparison shows an almost perfect agreement. The small difference between both is mainly due to the finite time window considered in the simulations and small leakage errors in the estimation of the PSD.
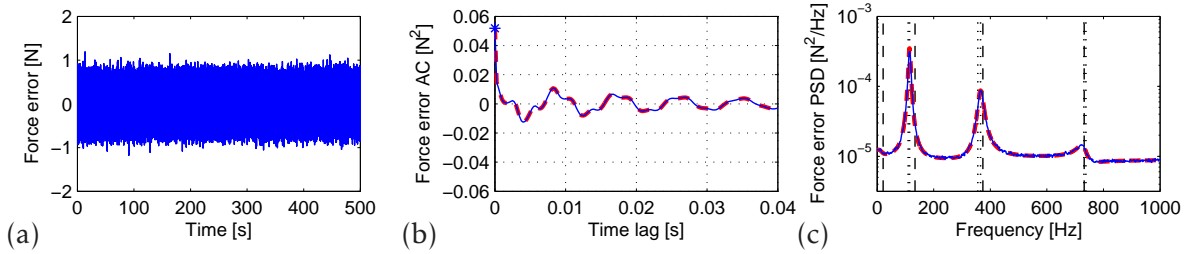
Figure 9: (a) Time history, (b) sample AC function (blue solid line) and AC function obtained from analytical expressions (red dashed line), and (c) sample PSD function (blue solid line) and PSD function obtained from analytical expressions (red dashed line) of the error on the estimated force $\hat{p}$, for white noise stochastic excitation. The undamped natural frequencies are indicated by vertical dashed lines in (c). The antiresonance frequencies of the transfer functions $H_{\mathrm{dp}}(\omega)$ that relate the Fourier transform of acceleration a_9 and displacement d_4 to the Fourier transform of the force p are indicated by vertical dotted lines in (c).

Tables 1 and 2 compare the estimated steady state error variance of the estimated force $\hat{p}$ ($P_{\mathrm{p}}^{\mathrm{ss}}$) and acceleration $\hat{a}_{11}$ ($P_{\mathrm{d_e}}^{\mathrm{ss}}$), respectively, to the mean squared errors obtained from the numerical simulations, and the AC of the errors for time lag $l = 0$ ($R_{\tilde{p}\tilde{p}}[0]$ and $R_{\tilde{d}_e\tilde{d}_e}[0]$). For the present case of white noise stochastic excitation, both the error variance and the AC of the errors for a time lag $l = 0$ give the true variance of the errors on the estimated quantities, as already indicated in Section 2.4.

Colored noise stochastic excitation Figures 11 and 12 show the time history, the sample AC and PSD function of the error on the estimated force $\hat{p}$ and the estimated acceleration $\hat{a}_{11}$, respectively, as obtained from the numerical simulations. The figures also compare the sample AC and PSD function of the error on the estimated quantities to the AC and PSD obtained from Eqs. (19), (62), and (64). As in the previous case of white noise stochastic excitation, the comparison shows an almost perfect agreement. The AC of the error on both estimated quantities again shows a significant correlation with time.

Tables 1 and 2 compare the estimated steady state error variance of the estimated force $\hat{p}$ ($P_{\mathrm{p}}^{\mathrm{ss}}$) and acceleration $\hat{a}_{11}$ ($P_{\mathrm{d_e}}^{\mathrm{ss}}$), respectively, to the mean squared errors ob-
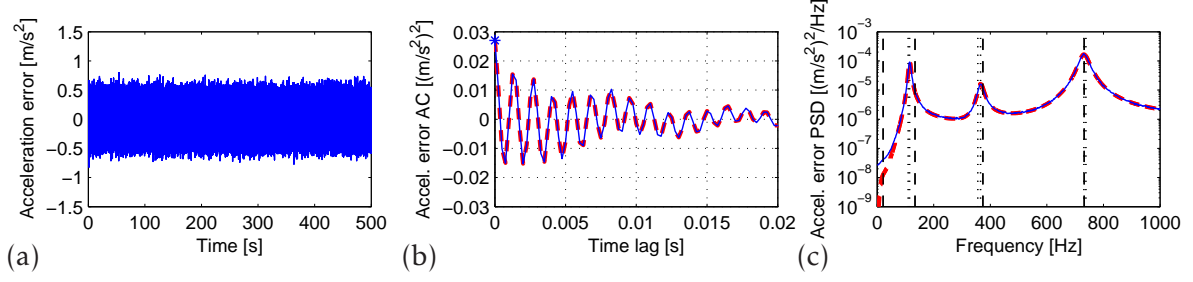
Figure 10: (a) Time history, (b) sample AC function (blue solid line) and AC function obtained from analytical expressions (red dashed line), and (c) sample PSD function (blue solid line) and PSD function obtained from analytical expressions (red dashed line) of the error on the estimated acceleration $\hat{a}_{11}$, for white noise stochastic excitation. The undamped natural frequencies are indicated by vertical dashed lines in (c). The antiresonance frequencies of the transfer functions $H_{dp}(\omega)$ that relate the Fourier transform of acceleration a_9 and displacement d_4 to the Fourier transform of the force p are indicated by vertical dotted lines in (c).

tained from the numerical simulations, and the AC of the errors for time lag $l = 0$ ($R_{\tilde{p}\tilde{p}[0]}$ and $R_{\tilde{d}_e\tilde{d}_e[0]}$). For colored noise stochastic excitation, the error covariance matrices obtained from the joint input-state estimation algorithm do not present the true error variance, since the white noise assumption is violated. The true value of the variance of the errors on the estimated quantities if found, however, from the AC of the errors for a time lag $l = 0$, as computed in Section 2.4.

Stochastic loads	P_p^{ss}	$\frac{1}{N}\sum_{k=1}^{N} \tilde{p}_{[k|k]}^2$	$R_{\tilde{p}\tilde{p}[0]}$
White noise	5.18×10^{-2} N^2	5.18×10^{-2} N^2	5.18×10^{-2} N^2
Colored noise	1.17×10^1 N^2	1.27×10^1 N^2	1.28×10^1 N^2

Table 1: Comparison of the steady state error variance of the estimated force $\hat{p}$ (P_p^{ss}), the mean squared force error obtained from the numerical simulations ($\frac{1}{N}\sum_{k=1}^{N} \tilde{p}_{[k|k]}^2$), and the AC of the force error for time lag $l = 0$ ($R_{\tilde{p}\tilde{p}[0]}$).

Stochastic loads	$P_{d_e}^{ss}$	$\frac{1}{N}\sum_{k=1}^{N} \tilde{d}_{e[k|k]}^2$	$R_{\tilde{d}_e\tilde{d}_e[0]}$
White noise	2.69×10^{-2} (m/s^2)^2	2.69×10^{-2} (m/s^2)^2	2.69×10^{-2} (m/s^2)^2
Colored noise	6.35 (m/s^2)^2	2.67 (m/s^2)^2	2.67 (m/s^2)^2

Table 2: Comparison of the estimated steady state error variance of the estimated extrapolated acceleration $\hat{a}_{11}$ ($P_{d_e}^{ss}$), the mean squared acceleration error obtained from the numerical simulations ($\frac{1}{N}\sum_{k=1}^{N} \tilde{d}_{e[k|k]}^2$), and the AC of the acceleration error for time lag $l = 0$ ($R_{\tilde{d}_e\tilde{d}_e[0]}$).

The previous calculations show that the uncertainty on the estimated force, the system states, and the extrapolated response, can be quantified by means of their PSD and AC function, assuming the PSD function of the (stationary) measurement errors and stochastic forces to be known. The uncertainty quantification approach can be used next to design a sensor network which minimizes the uncertainty on the estimated quantities, and to determine the optimal noise statistics that are applied for joint input-state estimation (see also [6]).
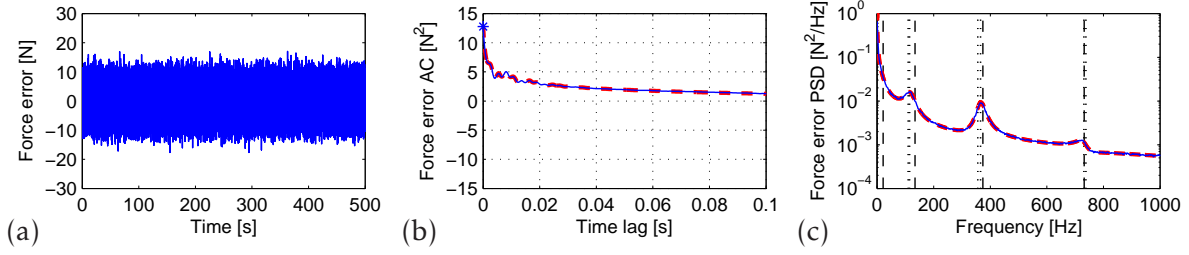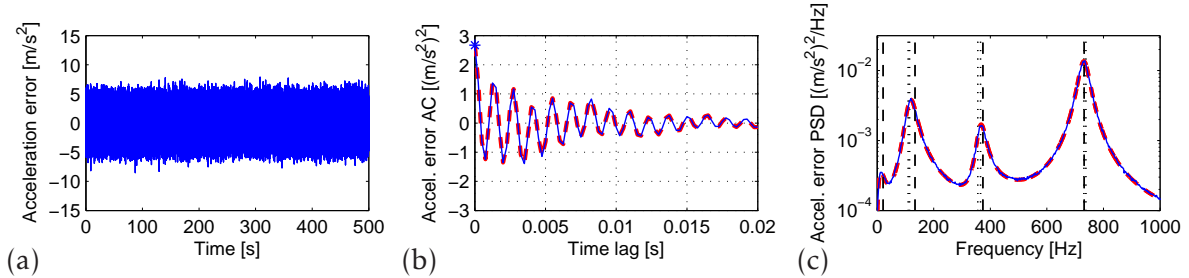
Figure 11: (a) Time history, (b) sample AC function (blue solid line) and AC function obtained from analytical expressions (red dashed line), and (c) sample PSD function (blue solid line) and PSD function obtained from analytical expressions (red dashed line) of the error on the estimated force $\hat{p}$, for colored noise stochastic excitation. The undamped natural frequencies are indicated by vertical dashed lines in (c). The antiresonance frequencies of the transfer functions $H_{\mathrm{dp}}(\omega)$ that relate the Fourier transform of acceleration a_9 and displacement d_4 to the Fourier transform of the force p are indicated by vertical dotted lines in (c).

Figure 12: (a) Time history, (b) sample AC function (blue solid line) and AC function obtained from analytical expressions (red dashed line), and (c) sample PSD function (blue solid line) and PSD function obtained from analytical expressions (red dashed line) of the error on the estimated acceleration $\hat{a}_{11}$, for colored noise stochastic excitation. The undamped natural frequencies are indicated by vertical dashed lines in (c). The antiresonance frequencies of the transfer functions $H_{\mathrm{dp}}(\omega)$ that relate the Fourier transform of acceleration a_9 and displacement d_4 to the Fourier transform of the force p are indicated by vertical dotted lines in (c).

4   CONCLUSIONS

This paper presents a method for quantification of the uncertainty on the results obtained from joint input-state estimation, introduced by measurement errors and unknown stochastic excitation, that is acting on the structure besides the forces that are to be identified. Numerical simulations show that the uncertainty on the estimated force, the system states, and the extrapolated response, can be quantified by means of their power spectral density and autocorrelation function, assuming the power spectral denity function of the (stationary) measurement errors and stochastic forces to be known. The uncertainty quantification approach can be used to design a sensor network which minimizes the uncertainty on the estimated quantities, and to determine the optimal noise statistics that are applied for joint input-state estimation.

REFERENCES

[1] G.F. Franklin, J.D. Powell, and M. Workman. *Digital control of dynamic systems*. Addison-Wesley, Menlo Park, CA, third edition, 1998.

[2] S. Gillijns and B. De Moor. Unbiased minimum-variance input and state estimation for linear discrete-time systems with direct feedthrough. *Automatica*, 43(5):934–937, 2007.

[3] E.M. Hernandez. A natural observer for optimal state estimation in second order linear structural systems. *Mechanical Systems and Signal Processing*, 25(8):2938–2947, 2011.

[4] E. Lourens, C. Papadimitriou, S. Gillijns, E. Reynders, G. De Roeck, and G. Lombaert. Joint input-response estimation for structural systems based on reduced-order models and vibration data from a limited number of sensors. *Mechanical Systems and Signal Processing*, 29:310–327, 2012.

[5] K. Maes, E. Lourens, K. Van Nimmen, E. Reynders, G. De Roeck, and G. Lombaert. Design of sensor networks for instantaneous inversion of modally reduced order models in structural dynamics. *Mechanical Systems and Signal Processing*, 52–53:628–644, 2014.

[6] K. Maes, A.W. Smyth, G. De Roeck, and G. Lombaert. Joint input-state estimation in structural dynamics. *Mechanical Systems and Signal Processing*, 2015. Submitted for publication.

[7] Y. Niu, M. Klinkov, and C.-P. Fritzen. Online force reconstruction using an unknown-input Kalman filter approach. In *Proceedings of the 8th International Conference on Structural Dynamics, EURODYN 2011*, pages 2569–2576, Leuven, Belgium, 2011.

[8] C. Papadimitriou, C.-P. Fritzen, P. Kraemer, and E. Ntotsios. Fatigue predictions in entire body of metallic structures from a limited number of vibration sensors using Kalman filtering. *Structural Control and Health Monitoring*, 18(5):554 –573, 2011. Published online in Wiley InterScience (www.interscience.wiley.com). DOI:10.1002/stc.395.

[9] E. Parloo, P. Verboven, P. Guillaume, and M. Van Overmeire. Force identification by means of in-operational modal models. *Journal of Sound and Vibration*, 262(1):161–173, 2003.

[10] B. Peeters and G. De Roeck. Reference-based stochastic subspace identification for output-only modal analysis. *Mechanical Systems and Signal Processing*, 13(6):855–878, 1999.

[11] E. Reynders and G. De Roeck. Reference-based combined deterministic-stochastic subspace identification for experimental and operational modal analysis. *Mechanical Systems and Signal Processing*, 22(3):617–637, 2008.

[12] M. Shinozuka and G. Deodatis. Simulation of stochastic processes by spectral representation. *Applied Mechanics Reviews*, 44(4):191–204, 1991.

[13] P. Van Overschee and B. De Moor. Subspace algorithm for the stochastic identification problem. *Automatica*, 29(3):649–660, 1993.